Journal of Engineering and Applied Sciences 14 (9): 2813-2821, 2019
ISSN: 1816-949X
© Medwell Journals, 2019

Exergy Analysis of Solar LiBr-H_2O Absorption System for Cooling a Building

Abdulrahman Th. Mohammad
Baqubah Technical Institute, Middle Technical University (MTU), Baghdad, Iraq

Abstract: In this study, a computational routine using MATLAB based on the exergy method is developed to determine the exergy loss of LiBr-H_2O absorption system for cooling that was designed to cool a small building located in University Kebangsaan Malaysia. The performance parameters of the system including the coefficient of performance, the Carnot coefficient of performance, the exergetic efficiency and the efficiency ratio are computed at different operating temperatures. The effects of the main operating conditions on the performance parameters and the non-dimensional exergy loss of the whole system are presented. The results showed that the biggest part exergy losses in the system are in the solar collector and the absorber, regardless of operating conditions. The sum of the exergy losses of these two components is 54%, there by indicating that the designs for the collector and absorber are the most important components of the cycle.

Key words: Solar, exergy loss, absorption refrigeration, building, important components, collector and absorber

INTRODUCTION

In a cooling system that consists of several adiabatic process components such as expansion valves and heat exchangers an energy balance might lead to conclude that these components are free of loss. For instance, conducting an energy balance on an expansion device could prove the occurrence of energy loss. However, after the expansion process the lower pressure reduces the usable research potential or exergy. For this reason, exergy analysis is the important tool for analyzing losses in complicated systems such as SAARS or power plants. The exergy concept has been extensively detailed in literature and a number of studies have used the exergy method to analyze the single-effect absorption refrigeration systems. Chua *et al.* (2002) modeled a single-stage absorption chiller using ammonia-water. They found that the biggest part of dissipation occurs in the rectifier. An absorption refrigeration cycle using LiBr-water was studied by Talbi and Agnew (2000) using the exergy concept; they calculated the exergy losses of each component. Lee and Sherif (2001) used exergy analysis to study multi-stage lithium bromide-water ARSs. The second law efficiency of the absorption chillers was computed from the thermodynamic properties, the entropy generation and exergy rate of the working fluids (Sencan *et al.*, 2005) carried out an exergy analysis of a single-effect absorption cooling system for cooling and heating applications. They presented the difference in the coefficients of performance and exergy efficiency that depended on the temperature of generator and chilled water. A dynamic simulation of a single-effect LiBr-H_2O absorption chiller considering the effects of thermal masses of main components and exergetic efficiency is performed (Iranmanesh and Mehrabian, 2013). The results showed that the heat transfer rates generator and condenser are highly dependent of thermal mass of the condenser whereas the heat transfer rates of evaporator and absorber are hardly affected by thermal masses. The amount of COP, heat transfer of both generator and condenser and the exergetic efficiency can be improved when the effects of all thermal masses are regarded simultaneously. By Avanessian and Ameri (2014) study, the energy and exergy analysis have been used for cooling systems including hot-water single-effect, hot-water double-effect or direct-fired double-effect LiBr-H_2O absorption chillers. The Results showed that the total exergy efficiency increases with increasing the generator or ambient air temperature, decreases with increasing the evaporator temperature and changes slightly with relative humidity. The single-effect system is uneconomical and the payback period in the case of utilizing the direct-fired double-effect chiller instead of the hot-water is about 3.5 years. Other studies of Fartaj (2004), Gomri and Hakimi (2008), Khaliq and Kumar (2008), Martinez and Rivera (2009) focused on double-effect absorption cooling systems using exergy analysis. However, few research based on exergy method focused on SAARS. For example, Ravikumar *et al.* (1998) carried out a study on a solar-assisted double effect absorption cooling system using exergy analysis and presented the effect of operating temperature in generator 1 and 2 on

exergy values. Hasan *et al*. (2002) conducted an analysis of the first and second laws of power and refrigeration cycle driven by solar energy. Their study defined the second law efficiency as relative to a reversible cycle and then maximized this efficiency to determine the optimum operating conditions of the system. The performance of a cycle was investigated over a heat source temperature range of 330-470 K. Ezzine *et al*. (2004) carried out a study on a double effect solar-assisted absorption refrigeration system. They quantified the irreversibility of all components in the chiller and then calculated the potential contribution of each individual component to the energy efficiency of the overall system. Onan *et al*. (2010) carried out a study on a solar-assisted absorption cooling system using exergy analysis. They determined the hourly exergy loss values of all components and they observed that the highest exergy losses are in the solar collector and generator. Past exergy studies have not focused on the annual total exergy destruction for SAARSs. In this study, a thermodynamic analysis as well as first and second Law analyses of a SAAR was conducted. The effects of exergy loss and non-dimensional exergy loss of all components as well as their contributions to the overall exergy loss are determined using MATLAB. Additionally, the annual total exergy destruction of each component is presented.

MATERIALS AND METHODS

System description: The schematic diagram of the proposed SAAR system that located in University Kebangsaan Malaysia is shown in Fig. 1. The SAARS consists of a solar collector subsystem and an absorption refrigeration subsystem using LiBr-H_2O as a working fluid. The major components of the system are the solar collector (sc), generator (gen), absorber (abs), condenser (cond), evaporator (evp), pump (p), expansion Valves (V1 and V2) and a Solution Heat exchanger (SHX). Q_{gen} is the heat input rate from the heat source by solar energy to the generator (17-21), Q_{cond} and Q_{abs} are the heat rejection rates from the condenser and the absorber to the cooling tower, respectively (11-14) and Q_{evp} is the heat input rate from the cooling load (15-16) to the evaporator. The vapor refrigerant coming from the evaporator (10) is absorbed by a strong lithium liquid solution (6). The liquid solution is then pumped through the SHX (1-3). The refrigerant is boiled out of the solution through the addition of heat. Subsequently, the refrigerant goes into the condenser (7-8) and the evaporator through the expansion Valve (V1). Finally, the strong lithium liquid solution returns back to the absorber through the SHX and the solution reducing Valve (V2) (4-6).

To meet the thermal load of the generator, we calculated the one-year solar energy assistance system performance of a small building located in University Kebangssan Malaysia (UKM) and then used the data in the simulation. An absorption chiller driven by hot water with a cooling capacity of 40 kW was used to cool the building during the year. Environmental temperature variations are shown in Fig. 2 and hourly solar radiation values are given in Fig. 3. These values were taken from the Malaysian State Meteorological Center. The maximum environmental temperature was 27.7°C in April whereas the minimum was 25.8°C in November. Solar radiation was

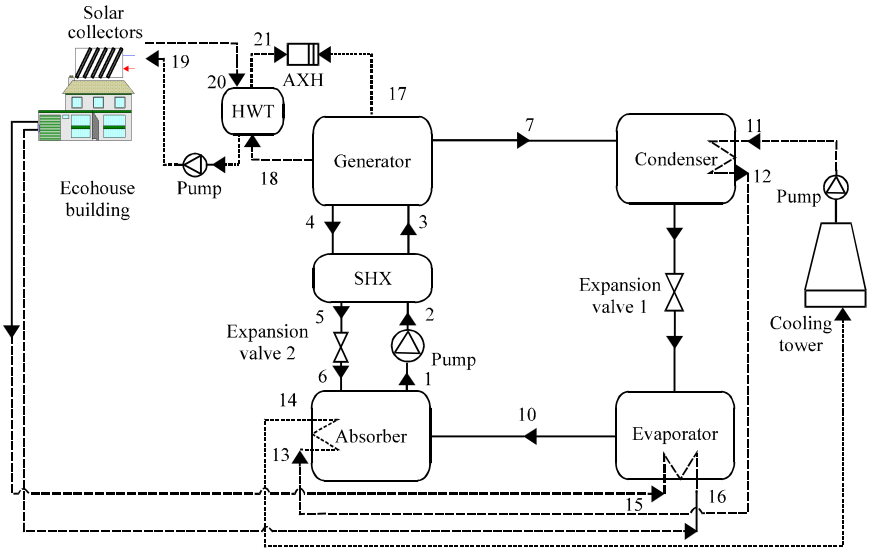

Fig. 1: Schematic of a SAARS design for use in cooling a building

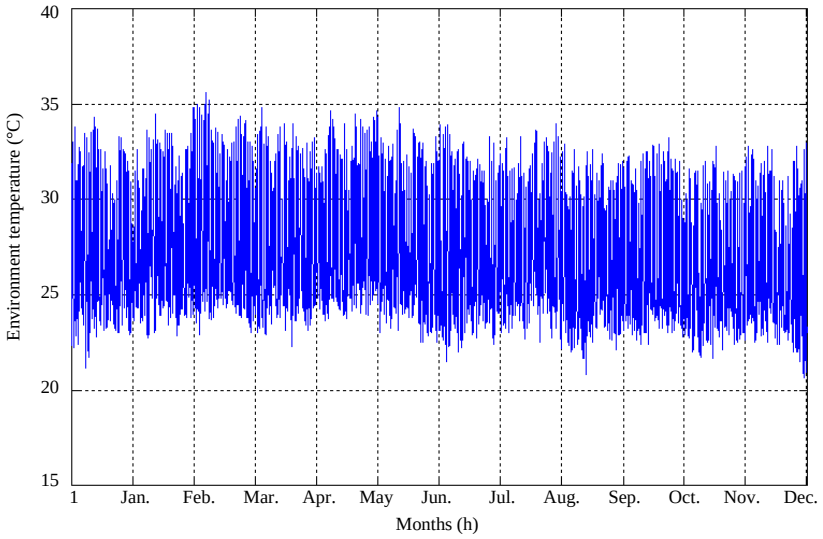

Fig. 2: Variations in environmental temperatures throughout the year (°C)

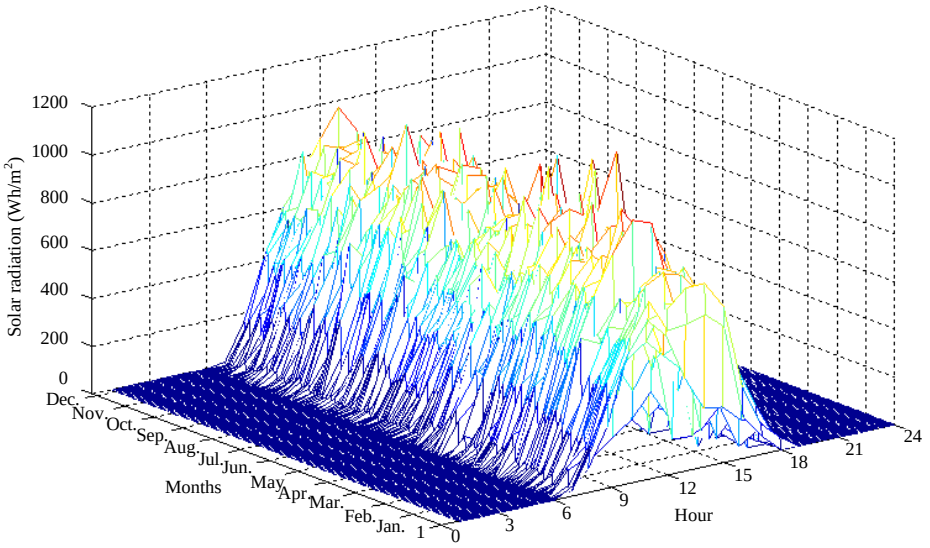

Fig. 3: Solar radiation data during the year (Wh/m^2)

about 16 MJ/m^2 all year round and the maximum solar radiation was obtained in March and April. The minimum solar radiation was obtained in November. A collector was installed at a slope of 15° facing north (γ = 0°). The fluid supplied from the solar collector may be heated even more in an Auxiliary Heater (AXH) and then goes to generator. The hourly variations in the useful energy of the collector during the year are shown in Fig. 4. Solar energy gain changed according to the Sun angles, hour area of collector and irradiation. As a dynamic system design, the utilization rate of the sun for every hour is important as it provides a balance between the requirement of the system and energy consumption throughout the year.

Thermodynamic analysis: As shown in Fig. 1, the equations of energy balance of the SAARS components can be written as follows:

$$\dot{Q}_u = \dot{m}_{20}\left(h_{20}-h_{19}\right) \quad (1)$$

$$\dot{Q}_{hwt} = \dot{m}_{18}\left(h_{18}-h_{19}\right) \quad (2)$$

$$\dot{Q}_{axh} = \dot{m}_{17}\left(h_{17}-h_{21}\right) \quad (3)$$

$$\dot{Q}_{gen} = \dot{m}_4 h_4 + \dot{m}_7 h_7 - \dot{m}_3 h_3 \quad (4)$$

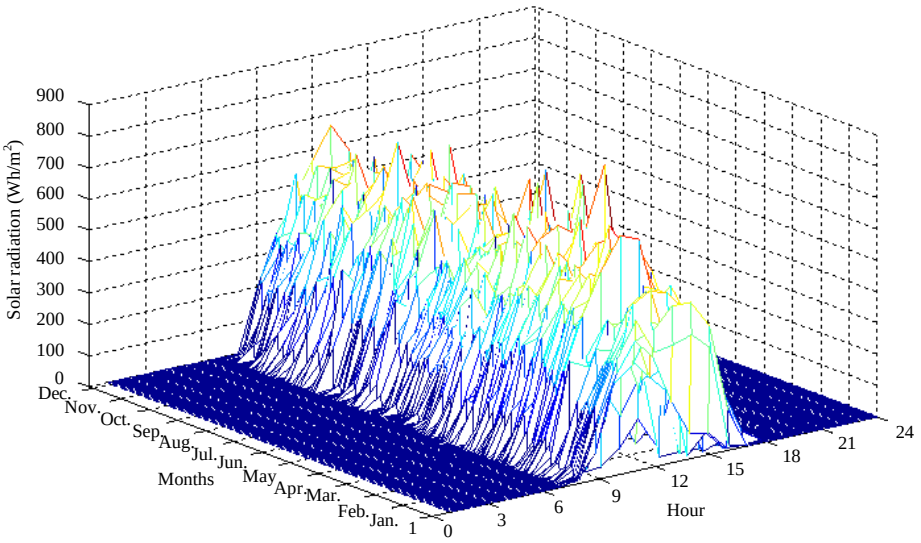

Fig. 4: Solar collector energy gain (Wh/m^2)

$$\dot{Q}_{cond} = \dot{m}_7 (h_7 - h_8) \quad (5)$$

$$\dot{Q}_{abs} = \dot{m}_6 h_6 + \dot{m}_{10} h_{10} - \dot{m}_1 h_1 \quad (6)$$

$$\dot{Q}_{evp} = \dot{m}_{10} (h_{10} - h_9) \quad (7)$$

$$\dot{W}_p = \dot{m}_2 (h_2 - h_1) = \frac{\dot{m}_1 v_1 (p_2 - p_1)}{\eta_p} \quad (8)$$

$$\dot{Q}_{SHX} = \dot{m}_4 (h_4 - h_5) = \dot{m}_3 (h_3 - h_2) \quad (9)$$

The exergy content of a pure substance is generally defined as:

$$e = (h - h_o) - T_o (s - s_o) \quad (10)$$

The terms h_o and s_o represent the enthalpy and entropy values, respectively, at the environmental temperature T_o which ultimately forms the energy (heat) sink for all irreversible and reversible processes. The exergetic balance that is applied to a fixed control volume can be written as the following equation (Bejan *et al*., 1996):

$$\sum \dot{m}_i e_i - \sum \dot{m}_o e_o + \dot{Q}\left(1 - \frac{T_o}{T}\right) - \dot{W} - \dot{E}_d = 0 \quad (11)$$

The first two terms are the sum of the exergy input and output flow rates, respectively. The third term is the exergy of heat $\dot{Q}$ which is transferred at a constant temperature T and it is positive if it is inside the system. $\dot{W}$ is the mechanical research transfer to or from the system and the last term $\dot{E}_d$ is exergy destroyed due to internal irreversibilities. For each component of SAARS, the equation of exergy loss rate can be determined as follows:

$$\Delta\dot{E}_{sc} = \dot{m}_{19}(e_{19} - e_{20}) + \dot{Q}_{rad}\left(1 - \frac{T_o}{T_{sc}}\right)) \quad (12)$$

$$\Delta\dot{E}_{hwt} = \dot{m}_{18} e_{18} + \dot{m}_{20} e_{20} - \dot{m}_{19} e_{19} - \dot{m}_{21} e_{21} \quad (13)$$

$$\Delta\dot{E}_{axh} = \dot{m}_{21}(e_{21} - e_{17}) + \dot{Q}_{axh}\left(1 - \frac{T_o}{T_{axh}}\right) \quad (14)$$

$$\Delta\dot{E}_{gen} = \dot{m}_3 e_3 + \dot{m}_{17} e_{17} - \dot{m}_4 e_4 - \dot{m}_7 e_7 - \dot{m}_{18} e_{18}) \quad (15)$$

$$\Delta\dot{E}_{cond} = \dot{m}_7 e_7 + \dot{m}_{11} e_{11} - \dot{m}_8 e_8 - \dot{m}_{12} e_{12} \quad (16)$$

$$\Delta\dot{E}_{abs} = \dot{m}_6 e_6 + \dot{m}_{10} e_{10} + \dot{m}_{13} e_{13} - \dot{m}_1 e_1 - \dot{m}_{14} e_{14} \quad (17)$$

$$\Delta\dot{E}_{evp} = \dot{m}_9 e_9 + \dot{m}_{15} e_{15} - \dot{m}_{10} e_{10} - \dot{m}_{16} e_{16} \quad (18)$$

$$\Delta\dot{E}_p = \dot{m}_1 e_1 - \dot{m}_2 e_2 + \dot{W}_p \quad (19)$$

$$\Delta\dot{E}_{SHX} = \dot{m}_4 e_4 + \dot{m}_2 e_2 - \dot{m}_3 e_3 - \dot{m}_5 e_5 \quad (20)$$

$$\Delta\dot{E}_{V1} = \dot{m}_8 (e_8 - e_9) \quad (21)$$

$$\Delta\dot{E}_{V2} = \dot{m}_5 (e_5 - e_6) \quad (22)$$

The total exergy loss rate of the SAARS is the sum of the exergy loss rate in each component, therefore:

$$\Delta \dot{E}_{tot} = \sum_{i=1}^{N} \Delta \dot{E}_i \quad (23)$$

where, N represents the number of components in the SAARS. The ratio of exergy loss rate in each individual component to the total exergy loss rate of the present system is defined as the non-dimensional exergy loss of the component. The non-dimensional exergy loss of each component is expressed as follows:

$$\psi_i = \frac{\Delta \dot{E}_i}{\Delta \dot{E}_{tot}} \quad (24)$$

Performance parameters that are used to measure the performance of refrigeration systems, including the Coefficient of Performance (COP), the exergetic Efficiency (ECOP), the efficiency ratio (η) and carnot Coefficient of Performance (COP_c) are written as follows (Sozen, 2001, Bejan, 2006):

$$COP = \frac{\dot{Q}_{evp}}{\dot{Q}_{gen} + \dot{W}_p} \quad (25)$$

$$ECOP = \frac{-\dot{Q}_{evp}\left(1-\frac{T_o}{T_{evp}}\right)}{\dot{Q}_{gen}\left(1-\frac{T_o}{T_{gen}}\right)+\dot{W}_p} \quad (26)$$

$$\eta = \frac{COP}{COP_c} \quad (27)$$

$$COP_c = \left(\frac{T_{gen}-T_{abs}}{T_{gen}}\right)\left(\frac{T_{evp}}{T_{cond}-T_{evp}}\right) \quad (28)$$

For the absorption refrigeration cycle, the theoretical calculations of performance parameters were conducted using the known values of T_{gen}, T_{evp}, T_{cond} and T_{abs}. The COP, COP_c, ECOP and η values as well as the concentrations of the solution in the generator and absorber were calculated for the following ranges of temperatures: in the generator at 75 and 100°C in the condenser at 35 and 45°C with the absorber temperature assumed to be the same as the condenser temperature and at the evaporator from 3-15°C. For purposes of analysis, the following assumptions are made:

- The system is in a steady state
- The temperatures of the condenser, absorber, evaporator and generator are constant and uniform throughout the components
- The expansion process in the expansion device is at constant enthalpy
- The reference environmental conditions for the system are T_o = 25°C and p_o = 1 atm
- The condenser and absorber cooling water temperatures at the inlet and exit are assumed to be equal to T_{cond}-15-10°C, respectively
- The water to be chilled enters the evaporator at T_{evp+}15°C and leaves at T_{evp}+7°C
- Cooling capacity is 40 kW

The average heat removal factor and heat loss coefficient for the evacuated tube solar collector of $F_R(\tau\alpha)$ = 0.8 and F_RUL = 2.0 W/m^2.K, respectively are used.

The thermodynamic properties of the LiBr-H_2O mixture were taken from the correlations provided by (Patek and Klomfar, 2006). The liquid water and vapor properties were determined using the equations by (Talbi and Agnew, 2000).

RESULTS AND DISCUSSION

A computational routine using MATLAB and based on exergy method was used to calculate the thermodynamic properties, mass flow rate and concentration exergy at all state points of the absorption system. The results are presented in Table 1. The simulation results of the first law analysis of the system are listed in Table 2. The input parameters of simulation were taken as T_{gen} = 90°C, T_{evp} = 5°C, T_{cond} = 35°C, η_p = 95% and ϵ_{SHX} = 70%. The absorber temperature was taken to be equal to the condenser temperature. The cooling capacity was 40 kW. Solar radiation and collector areas of I = 700 W/m^2 and A_{sc} = 100 m^2, respectively were used. The highest thermal load occurred in the generator and the thermal load in the condenser was higher than that in the evaporator. These results could be attributed to the superheating property of the inlet water vapor in the condenser. The pump research was inconsiderable compared with the heat transfer rates of other components.

The second law analysis results of the SAARS are shown in Table 3. The solar collector had the highest exergy loss rate, followed by the absorber. As exergy loss rates in the expansion valves and pump were very small, their effects on the total exergy loss rate were considered insignificant. The non-dimensional exergy loss of all components is also presented in Table 3. The exergy losses of the solar collector and absorber proved to be important fractions of the total exergy loss in the whole system. Exergy loss in the solar collector was 31%

Table 1: Exergy and energy calculations of the system on April 24, 2013 at 12 pm

Points	T (C)	P (kPa)	h (kJ/kg)	s (kJ/kg.K)	(kg/sec)	x (kg/kg sol)	e (kJ/kg)
1	35.00000	0.872530	85.33132	0.211459	0.115373	0.552679	26.89534
2	34.91510	5.629057	85.36071	0.210905	0.115373	0.552679	27.08995
3	63.62980	5.629057	143.8671	0.392438	0.115373	0.552679	31.47214
4	90.00000	5.629057	239.5927	0.474778	0.098451	0.647679	102.6483
5	51.44057	5.629057	171.0296	0.274704	0.098451	0.647679	93.73699
6	51.32650	0.872530	171.0296	0.274085	0.098451	0.647679	93.92168
7	90.00000	5.629057	2669.26	8.663521	0.016923	0	90.842
8	35.00000	5.629057	146.7719	0.505139	0.016923	0	0.775291
9	34.93070	0.872530	146.7719	0.504200	0.016923	0	1.055223
10	05.00000	0.872530	2510.452	9.025099	0.016923	0	-175.771
11	20	2.339194	83.97154	0.296585	2.037801	0	0.155285
12	25	2.339194	104.9193	0.367330	2.037801	0	0.010357
13	20	2.339194	83.97154	0.296585	1.192059	0	0.155285
14	12	2.339194	50.41615	0.180646	1.192059	0	1.16713
15	20	2.339194	83.97154	0.296585	2.361907	0	0.155285
16	25	2.339194	104.9193	0.367330	2.361907	0	0.010357
17	96	87.771120	402.1425	1.260377	4.135861	0	30.97161
18	93	87.771120	389.5306	1.226058	4.135861	0	28.59204
19	95	84.608990	397.9374	1.248965	4.135861	0	30.16909
20	97.4498	84.608990	408.3826	1.276874	4.135861	0	32.29304
21	96	2.488096	402.1425	1.260377	4.135861	0	30.97161

Table 2: Energy transfer rates at various components and the performance parameters of the system

Components	Heat transfer rate (kW)
Solar collector (Q_u)	43.2
Hot water storage tank (Q_{hwt})	25.8
Auxiliary heater (Q_{axh})	0
Generator (Q_{gen})	52.161
Condenser (Q_{cond})	62.687
Absorber (Q_{abs})	49.477
Evaporator (Q_{evp})	40
Solution heat exchanger (Q_{SHX})	6.75
Pump ($\dot{W}_P$)	0.0034
Performance parameters of the SAARS	
Coefficient of Performance (COP)	0.767
Carnot coefficient of Performance (COP_c)	1.404
Exergetic efficiency (ECOP)	0.308
Efficiency ratio (τ)	0.546

Table 3: Exergy loss rates of the components

Components	Exergy loss rate $\Delta\dot{E}$ (kW)	Non-dimensional exergy loss (ψ %)
Solar collector	4.74	31
Hot water storage tank	1.1	7
Auxiliary heater	0	0
Generator	1.89	13
Condenser	1.72	11
Absorber	3.51	23
Evaporator	1.8	12
Solution heat exchanger	0.37	2
Pump	0.014	1
Expansion Valve (V_1)	0	0
Expansion Valve (V_2)	0	0
Total	15.1	100

whereas exergy loss in the absorber was 23%. The sum of exergy losses of these two components was 54% which is a remarkably high value. The biggest part of exergy loss occurred in the generator at any rate of operating conditions. Thus, the designs of the solar collector and absorber are the most important components of the cycle. Figure 5 and 6 show the exergy destruction distribution values of each component for specific hours in April 24

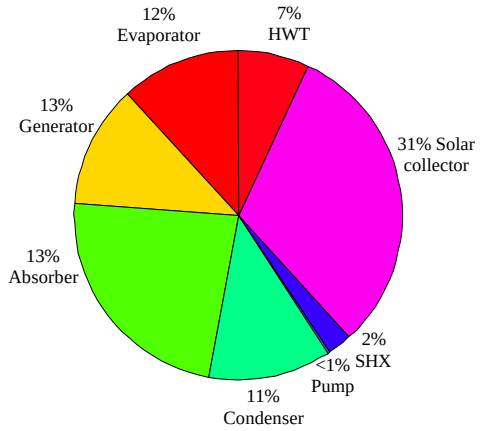

Fig. 5: Exergy destruction distribution of SAARS components at 12 pm on April 24, 2013

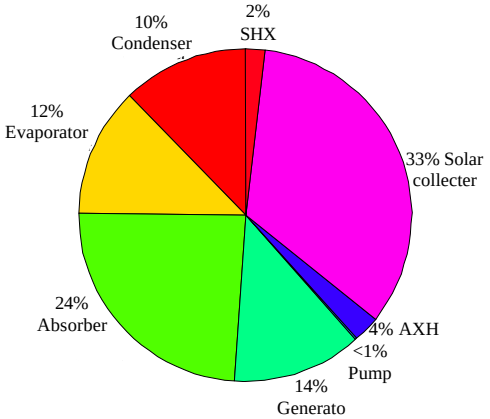

Fig. 6: Exergy destruction distribution of SAARS components at 1 am on November 21, 2013

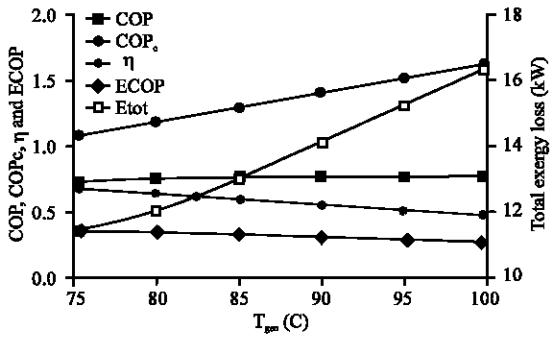

Fig. 7: Variation of performance parameters and total exergy loss at different generator temperature

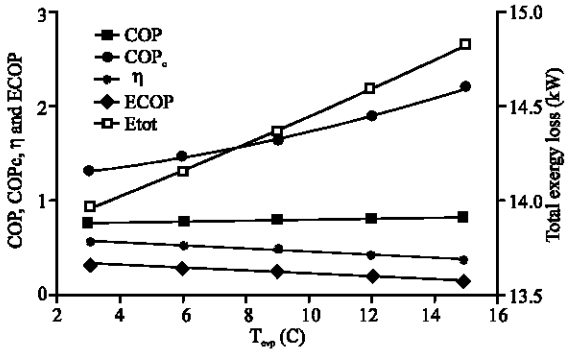

Fig. 8: Variation of performance parameters and total exergy loss at different evaporator temperature

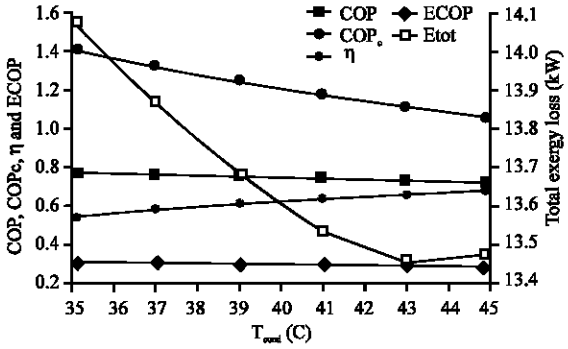

Fig. 9: Variations in the performance parameters and total exergy loss at different condenser temperatures

and November 21, respectively. These 2 days were selected because the supply temperature of the generator in the system at 12 pm on April 24 was obtained through the fluid supplied from solar collectors and waste heat was also stored. On the other word, the tank was not in use at 1 am on November 21 and the auxiliary heater was in circuit together with the collectors. The biggest part of total exergy loss of SAARS was found to originate from the solar collectors and absorber of the absorption chiller.

Figure 7 shows the variations of the performance parameters (COP, COP_c, ECOP and η) with the generator temperature at the same input conditions. The COP initially exhibited a significant increase with the increase in temperature of generator and then the slope of the performance curves became almost stable which suggested that increasing the generator temperature to a certain value does not provide much improvement for the COP.

Although, the values of the COP and ECOP were dissimilar, their trends were similar. Thus, both the COP and ECOP decreased with the increase in generator temperature. At higher generating temperatures, although, COP remained approximately stable, η gradually decreased. Furthermore, the COP_c value also increased under this temperature. The COP_c was significantly higher than that in the actual system performance which indicated that a large amount of loss occurred. This result may be attributed to the increase in generator temperature which negatively influenced the ECOP values as seen in Eq. 26. A higher generator temperature implied more external input exergy supplied to the cooling system. Thus, although, the latter could drive more water vapor from the solution to create cooling, it could also generate more exergy losses in the generator, condenser and absorber as their average temperatures rise. This effect would contribute negatively to the ECOP of the system.

Figure 8 shows variations in the performance parameters of the SAARS at different evaporator temperatures. The COP increased when the evaporator temperature increased. Unlike the COP, the ECOP of the absorption system decreased with the increase in evaporator temperature which may be explained by the definition of the second law of thermodynamics. The COP_c value also increased at a lower temperature. Figure 9 and 10 show the variations in the performance parameters of the SAARS with consideration for the condenser and absorber temperatures. In this case, both COP and ECOP decreased with the increase of the condenser and absorber temperatures. This behavior may be attributed to the increase of the pressure in the generator part when the condenser and absorber temperatures increase which would lead to the release of less water vapor from the generator. At the same time, lower condenser and absorber temperatures have a greater potential of creating a cooling effect at the same flow rate. In general, high COP values can be attained byoperating the cycle at low values of the circulation ratio which implies high values of T_{gen} and T_{evp} and low values of T_{cond} and T_{abs}.

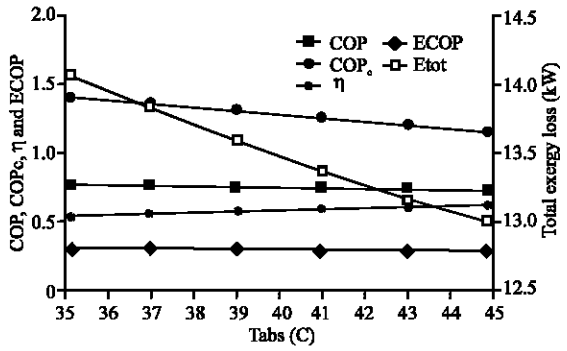

Fig. 10: Variations in the performance parameters and total exergy loss at different absorber temperatures

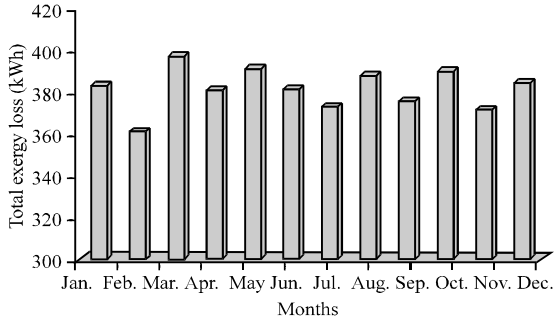

Fig. 11: Annual exergy destruction of the SAARS

Figure 11 indicates the annual total irreversibility of the SAARS. Based on the parameters such as environmental temperature and irradiation of the location of the ecohouse building, the heat gain of the building was found to increase in March and April, 2011. The increase in heat gain caused an increase in the irreversibility in the solar collector and its share with all components at an obvious rate. Generally as the heat gain of a building increases, the utilization of the collector also increases. Thus, the values of exergy loss in the solar energy assistance system and the other SAARS components also increased.

CONCLUSION

A SAARS designed to cool a building located in University Kebangssan Malaysia (UKM) was studied for an entire year by using the first and second laws of thermodynamics. The exergy loss of each component, total exergy loss of all components and performance parameters of the SAARS were calculated at different operating conditions by developing a simulation model programmed with MATLAB. The system operated with low condenser temperature yielded a higher cooling COP and a higher ECOP. The cooling system operating with relatively high evaporator temperatures had better COP and smaller ECOP than the one with low evaporator temperatures. Increasing the temperature of generator could enhance the COP of the SAARS. However, as the heat source temperature further increased, the performance of the system leveled off. This negative effect was found to be more dominant in the ECOP of the system, neglecting the benefits of a high heat source temperature. Furthermore, exergy losses in the solution heat exchanger, expansion valves and pump were very small fractions of the total exergy loss in the SAARS. Two components that obtained the highest exergy loss were the solar collector and the absorber. Thus, the designs of both the collector and absorber are the most important components of the cycle.

ACKNOWLEDGEMENTS

This study was supported by SERI (Solar Energy Research Institute) at University Kebangsaan Malaysia. The research are grateful to the staff of Baqubah Technical Institute/Middle Technical University and the staff of Engineering College/Diayla University for their help.

NOMENCLATURE

A = Area (m^2)
COP = Coefficient of Performance
e = e specific exergy (kJ/kg)
ECOP = Exergetic efficiency
$\dot{E}$ = Exergy rate (kW)
$\Delta\dot{E}$ = Exergy loss rate (kW)
h = Enthalpy (kJ/kg)
I = Hourly solar radiation (W/m^2)
$\dot{m}$ = Mass flow rate (kg/sec)
P = Pressure (kPa)
$\dot{Q}$ = Heat transfer rate (kW)
s = Entropy (kJ/kg.K)
$\dot{s}$ = Entropy generation rate (kW/K)
T = Temperature (°C)
v = Specific volume (m_3/kg)
$\dot{W}$ = Pump power (kW)
x = Lithium bromide mass fraction

Greek letters:

ϵ = Heat exchanger effectiveness
η = Efficiency ratio
γ = Surface azimuth angle
ψ = Non-dimensional exergy loss

Subscripts:

abs = Absorber
axh = Auxiliary heater
c = Carnot
cond = Condenser
d = Destruction
evp = Evaporator
gen = Generator
hwt = Hot water storage tank
I = Input, state point or index i = 1, 2, 3
j = Number of components
o = Ambient condition, output
p = Pump
sc = Solar collector
u = Useful
SHX = Solution heat exchanger
tot = Total
V = Expansion Valve

REFERENCES

Avanessian, T. and M. Ameri, 2014. Energy, exergy and economic analysis of single and double effect LiBr–H2O absorption chillers. Energy Build., 73: 26-36.

Bejan, A., 2006. Advanced Engineering Thermodynamics. 1st Edn., John Wiley and Sons, New York, ISBN: 978-0-471-67763-5.

Bejan, A., G. Tsatsaronis and M. Moran, 1996. Thermal Design and Optimization. John Wiley and Sons, New York, USA.

Chua, H.T., H.K. Toh and K.C. Ng, 2002. Thermodynamic modeling of an Ammonia-water absorption chiller. Intl. J. Refrig., 25: 896-906.

Ezzine, N.B., M. Barhoumi, K. Mejbri, S. Chemkhi and A. Bellagi, 2004. Solar cooling with the absorption principle: First and second law analysis of an Ammonia-water Double-generator absorption chiller. Desalin., 168: 137-144.

Fartaj, S.A., 2004. Comparison of energy, exergy and entropy balance methods for analysing Double-stage absorption heat transformer cycles. Intl. J. Energy Res., 28: 1219-1230.

Gomri, R. and R. Hakimi, 2008. Second law analysis of double effect vapour absorption cooler system. Energy Convers. Manage., 49: 3343-3348.

Hasan, A.A., D.Y. Goswami and S. Vijayaraghavan, 2002. First and second law analysis of a new power and refrigeration thermodynamic cycle using a solar heat source. Solar Energy, 73: 385-393.

Iranmanesh, A. and M.A. Mehrabian, 2013. Dynamic simulation of a Single-effect LiBr–H2O absorption refrigeration cycle considering the effects of thermal masses. Energy Build., 60: 47-59.

Khaliq, A. and R. Kumar, 2008. Exergy analysis of double effect vapor absorption refrigeration system. Intl. J. Energy Res., 32: 161-174.

Lee, S.F. and S.A. Sherif, 2001. Thermodynamic analysis of a lithium Bromide-water absorption system for cooling and heating applications. Intl. J. Energy Res., 25: 1019-1031.

Martinez, H. and W. Rivera, 2009. Energy and exergy analysis of a double absorption heat transformer operating with Water-lithium bromide. Intl. J. Energy Res., 33: 662-674.

Onan, C., D.B. Ozkan and S. Erdem, 2010. Exergy analysis of a solar assisted absorption cooling system on an hourly basis in villa applications. Energy, 35: 5277-5285.

Patek, J. and J. Klomfar, 2006. A computationally effective formulation of the thermodynamic properties of LiBr–H2O solutions from 273 to 500 K over full composition range. Intl. J. Refrig., 29: 566-578.

Ravikumar, T.S., L. Suganthi and A.A. Samuel, 1998. Exergy analysis of solar assisted double effect absorption refrigeration system. Renewable Energy, 14: 55-59.

Sencan, A., K.A. Yakut and S.A. Kalogirou, 2005. Exergy analysis of lithium bromide/water absorption systems. Renewable Energy, 30: 645-657.

Sozen, A., 2001. Effect of heat exchangers on performance of absorption refrigeration systems. Energy Convers. Manage., 42: 1699-1716.

Talbi, M.M. and B. Agnew, 2000. Exergy analysis: An absorption refrigerator using lithium bromide and water as working fluids. Applied Therm. Eng., 20: 619-630.